

FAST AND ACCURATE VISIBILITY COMPUTATION IN URBAN SCENES

Bruno Vallet and Erwann Houzay

Université Paris Est, IGN, Laboratoire MATIS
4, Av. Pasteur
94165 Saint Mandé Cedex, FRANCE
bruno.vallet@ign.fr (corresponding author), erwann.houzay@ign.fr
<http://recherche.ign.fr/labs/matis>

Working Groups I/2, III/1, III/4, III/5

KEY WORDS: Photogrammetry, Visibility, Mobile mapping, Building facade, Urban Scene

ABSTRACT:

This paper presents a method to efficiently compute the visibility of a 3D model seen from a series of calibrated georeferenced images. This is required to make methods aimed at enriching 3D models (finer reconstruction, texture mapping) based on such images scalable. The method consists in rasterizing the scene on the GPU from the point of views of the images with a known mapping between colors and scene elements. This pixel based visibility information is then made higher level by defining a set of geometric rules to select which images should be used when focusing on a given scene element. The visibility relation is finally used to build a visibility graph allowing for efficient sequential processing of the whole scene

1 INTRODUCTION

One of the most investigated applications of mobile mapping is the enrichment an existing 3D urban model (obtained from aerial photogrammetry for instance) with data acquired at the street level. In particular, the topics of facade reconstruction (Frueh and Zakhor, 2003) and/or texture mapping (Bénitez et al., 2010) have recently received a strong interest from the photogrammetry and computer vision communities. An important step in such applications is to compute the visibility of the scene, that is to answer to the questions:

- Which scene element is visible at a given pixel of a given image (pixel level)
- Which scene elements are seen well enough in a given image, i.e. for which scene elements does the image contain significant information (image level)

Depending on the applications, these questions can be asked the other way, that is querying the images/pixels seeing a given scene element or 3D point. In practice, mobile mapping generates a large amount of data, and an acquisition led on an average sized city will generate tens of thousands of images of tens of thousands of scene elements. In that case, a per pixel visibility computation based on ray tracing as done usually (Bénitez and Baillard, 2009) becomes prohibitively costly.

The first part of this paper proposes instead a visibility computation method taking advantage of the graphics hardware to make this computation tractable. Another problem arising in handling a large number of images acquired in an urban environment is that a given scene element might be seen at various distances and with various viewing angles during the acquisition. As a result, the set of images that view a given scene element will be heterogeneous, thus hard to handle in most applications. The second part of this paper tackles this issue by proposing appropriate geometric criteria in order to reduce this set to a more homogeneous one, and where the images contain substantial information about the scene element.

The contributions of this paper are twofold, and both aim at facilitating the exploitation of mobile imagery at large scale in urban areas:

- Fast per pixel visibility complex computation (Section 2)
- Quality aware and memory optimized image selection (Section 3)

Results are presented and discussed in Section 4, and conclusions and future works are detailed in Section 5.

1.1 Previous works

Enriching an existing 3D city model with ground based imagery is a quite important topic in photogrammetry (Haala, 2004), as well as a major application of mobile mapping systems (Bénitez et al., 2010). More precisely, the visibility computation method presented in this paper is designed to allow scalability of:

- Facade texture mapping methods: the images are used to apply a detailed texture to the facades of the model. This is especially important for 3D models built and textured from aerial images for which the facades textures are very distorted.
- Reconstruction from images: the images are used to build a detailed 3D model of objects of interest such as facades (Pénard et al., 2004) or trees (Huang, 2008). In this case, a careful selection of the images to input the reconstruction method should be made. This paper proposes an efficient approach to automatize this selection as long as a rough 3D model of the object to reconstruct is known (rectangle for a facade, sphere or cylinder for a tree), which is required to make such methods applicable to large scale reconstructions.

In most reconstruction/texture mapping work relying on mobile imagery, the problem of visibility computation is raised but often not explicitly tackled, so we guess that the image selection

is either made manually from visual inspection, probably using a GIS. Whereas this is sufficient to demonstrate the pertinence of a method, this becomes a major lock when considering scalability to an acquisition led over an entire city. In order to solve this problem, (Bénitez and Baillard, 2009) proposes and compares three approaches to visibility computation: 2D/3D ray tracing and Z buffering. The 2D approach is the fastest but the 2D approximation fails to give the correct visibility in all the cases when buildings are visible behind others, which frequently occurs in real situations. 3D ray tracing and Z buffering do not have this limitation but computation time is important even for a very sparse sampling of the solid angle of the image. This can be an issue as if too few rays are traced, scene elements seen by a camera may be missed. Moreover, this is insufficient to handle occlusions at the scale of a pixel.

As mentioned in (Bénitez et al., 2010), facade texture mapping calls for a per pixel visibility computation to take into account two kinds of occlusions: *predictable* occlusions that may be predicted by the model to texture (parts of the model hiding the facade to texture in the current view), and *unpredictable* occlusions. Unpredictable occlusions can be tackled based on laser and/or image (Korah and Rasmussen, 2008) information. Predictable occlusions require to compute visibility masks of the 3D objects to texture (Wang et al., 2002). Such per pixel visibility computation is extremely costly, and the purpose of this paper is to make it tractable. We achieve this by exploiting the GPU rendering pipeline, which is known to be much faster than the CPU as it is extremely optimized for that purpose, and is in fact much more adapted to our problem.

It should be mentioned that an alternative to visibility computation exists for 3D model enriching from ground data. It consists in constructing a textured 3D model from the ground data alone, then registering this ground based model to the 3D model to enrich. This is the preferred methodology in case laser scanning data was acquired simultaneously to the images. For instance, in (Frueh and Zakhor, 2003) and (Frueh and Zakhor, 2004) a ground based model is registered to the initial 3D city model based on Monte Carlo localization, then both models are merged. More recently, this was done based on images only with a reconstruction obtained by SLAM and registered by an Iterative Closest Point (ICP) method (Lothe et al., 2009). This could also be applied to the purely street side city modeling approach of (Xiao et al., 2009).

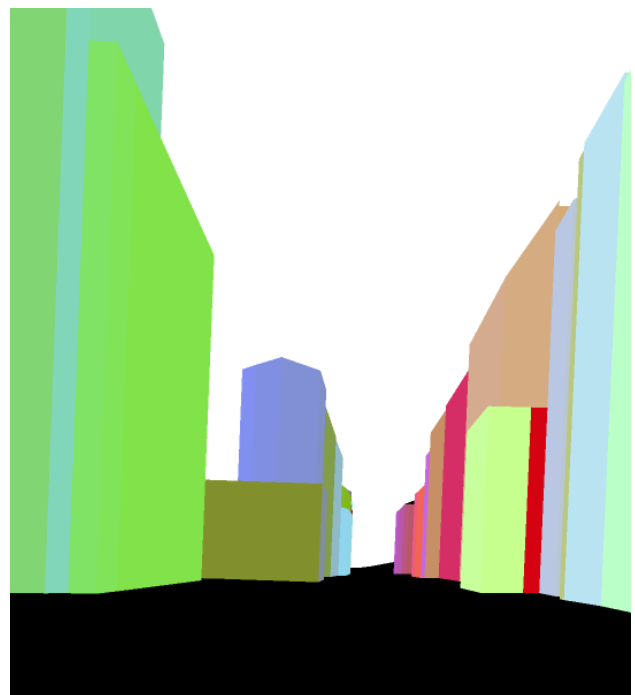
2 PIXELWISE VISIBILITY

This section presents the core of our method, which is to efficiently compute the visibility complex pixelwise by rasterization on the GPU. More precisely, we aim at finding which object of the 3D scene should be visible on each pixel of each acquired image. The obvious way to do that is to intersect the 3D ray corresponding to that pixel with the 3D scene, which is very costly even when optimizing this computation based on spatial data structures. In order to reduce computation time, we propose instead to rasterize the 3D scene from the viewpoint of each camera, that is to simulate the real life acquisition using the highly optimized rendering pipeline of the GPU. It relies on two successive steps:

1. Build a virtual camera in the 3D model accordingly to the extrinsic and intrinsic parameters of our real life camera (Section 2.1)
2. Perform a rasterization of the scene (see Fig. 1(b)) in a GPU buffer with a unique identifier per object of interest (Section 2.2).



(a) Real image



(b) Virtual image

Figure 1: A real image and superposable virtual image obtained by capturing the 3D model from the same point of view

2.1 Camera parameters transfer

Extrinsic parameters: Building an OpenGL camera simply requires to set the appropriate 4 by 4 matrix corresponding to the projective transform. However, special care should be taken as GPUs usually work in single precision floating point coordinates, as their development has always been driven by the games industry that focuses more on performance than on precision. This is completely incompatible with the use of geographic coordinates, and can lead to unacceptable imprecision during the rendering. A simple workaround is to choose a local frame centered within

the 3D scene, in which both the 3D model coordinates and the camera orientation will be expressed.

Intrinsic parameters: Calibration of a camera sets its intrinsic parameters consisting mainly in its focal, principal point of autocollimation (PPA) and inner distortion. Conversely, OpenGL relies on the notion of field of view (FOV), the PPA is always at the perfect center of the image and distortion cannot be applied. In most cases, the PPA is close enough to the image center for this to be negligible. If it is not, a larger image should be created containing the image to be rendered and with its center at the PPA, then cropped. Finally, the field of view should then be computed by:

$$FOV = 2 \cdot \tan^{-1} \left(\frac{\max(\text{width}, \text{height})}{2f} \right); \quad (1)$$

A simple means to handle the distortion is to resample the rendered image to make it finally perfectly superposable to the acquired one. Depending on the application, this resampling might not be necessary, and it might be more efficient to apply the distortion on the fly when a visibility information is queried. In both cases, the width and height of the rendered image should be chosen such that its distortion completely encompasses the acquired image.

2.2 Rasterization

The problem of *rendering* (generating virtual images of 3D scenes) has been widely studied in the computer graphics community, and two main methodologies have arisen:

1. **Rasterization** consists in drawing each geometric primitive of the scene using a depth buffer (also called Z-buffer) to know which primitive is in front of which from the current viewpoint.
2. **Ray tracing** consist in intersecting each 3D ray corresponding to a screen pixel with the scene, then iterating on reflected rays in order to define the appropriate color for that pixel.

Ray tracing is known to be much more expensive, but allows for very realistic lighting and reflexion effects. Ray tracing is also much harder to parallelize, such that GPUs always perform rendering by rasterization, making it extremely efficient and well suited in our case.

The result of a rasterization is a color image (the Z-buffer is also accessible if needed). Thus, the simplest way to get a visibility information from a rasterization is to give a unique color to each scene object of interest, and create a mapping between colors and scene objects. The only limitation to this method is that the number of objects of interests should not exceed the number of colors ($256^3 = 2^{24} \approx 16.8$ million) which in practice is completely sufficient (there are much less objects of interest such as facades or trees in the largest cities).

The second problem is that the size of the image to render might be arbitrarily larger than the size of the screen of the computer on which we will run the visibility computation. Hopefully, GPUs can perform *offline rendering*, that is to render a scene in a buffer of the GPU which size is only limited by the graphical memory (GRAM). This buffer can then be transferred to the RAM, and saved on the disk if required. Using lossless compression is strongly advised as colors now have an exact meaning that should

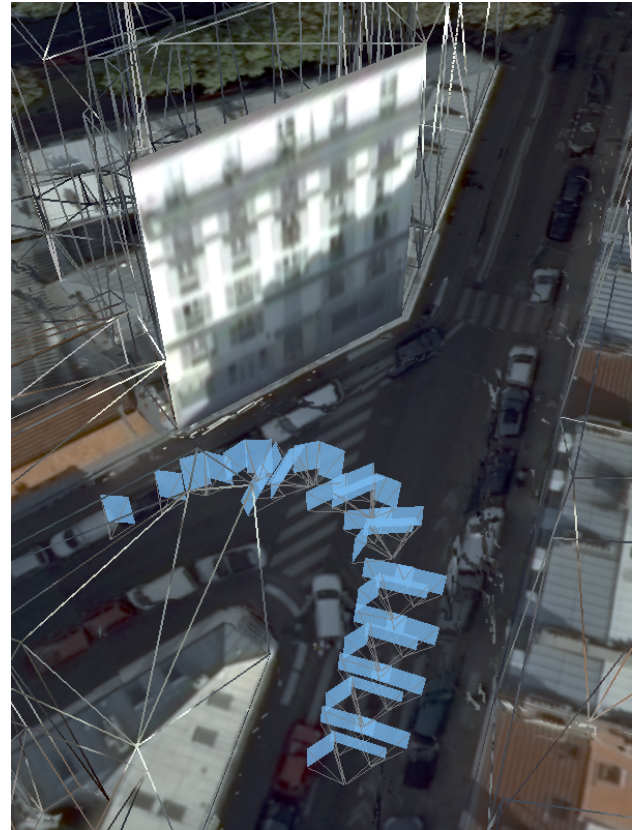


Figure 2: Set of images selected by our method as containing pertinent information about a facade (non wireframe)

absolutely be preserved, and most images rendered this way only present a limited number of colors arranged in large objects allowing for high lossless compression rates. In our experiments, the 1920x1080 buffers stored this way weighted 12 KBytes in average, which corresponds to a compression rate of 99.8%.

The result of this step, that we will call *visibility image* (Fig. 1), stores the direct visibility information, i.e. the answer to the question: Which is the object seen at a given pixel of a given image? Some more work still needs to be done in order to answer efficiently to the image level question: which objects are seen well enough in a given image? And the inverse one: which images see a given object well enough? The next section proposes a method to answer this questions that relies on a proper definition of the term "well enough" in this context.

3 PICTURE LEVEL VISIBILITY

Most reconstruction/texture mapping problems can be decomposed into one sub-problem for each scene element of interest. In this case, we need to be able to know which images will be useful to process the scene element in order to load them into the computer's memory. Loading too many will impair processing time and memory footprint, but it can even lower the quality of the result in some cases. This section tackles these problems in two steps:

1. Defining geometric criteria to select which images are useful for the processing.
2. Building a visibility graph to answer to inverse visibility queries.

Optionally, we will propose two applications of the visibility graph structure:

1. Optimizing the memory handling in sequential treatment.
2. Selecting a single sequence to avoid limit issues due to non static scene elements (shadows, mobile objects,...).

3.1 Geometric criteria

The first naive approach to determining the scene elements seen in an image is simply to build a list of all colors present in a visibility image, and declare the corresponding scene elements as viewed by the image. This is both inefficient and too simplistic. In fact, we want to select the images to use to process a scene element, so only the images seeing that element well enough should be used. Thus we propose two geometric criteria to select only the appropriate images:

1. **Image content:** The image should contain sufficient information about the scene element, or in other terms, the scene element should cover at least a certain portion of the visibility image. This criterion also has a practical aspect: we can accelerate the color counting by only checking the colors of a small sparse subset of the image. For instance, if the criterion corresponds to 10 000 pixels, checking only every 1 000 pixel is sufficient, provided that the sampling is homogeneous enough, and the criterion becomes having at least 10 samples of a given color. This will accelerate the pixel counting without impairing the result.
2. **Resolution:** The size of the pixel projected on the scene element should not exceed a given value (say $25cm^2$) or a given multiple (say 5 times) of the smallest projected pixel size. We estimate this projected pixel size at the barycenter of the projection of the scene element in the visibility image (this can be done simultaneously to the color counting, using the same sparse sampling). This criterion penalizes both distance and bad viewing angles.

These criteria should be sufficient for most applications, but they can be adapted if needed. An example of the set of images selected for a given scene element (facade) based on these criteria is shown on Fig. 2.

3.2 The visibility graph

The geometric criteria cited above establish a relation: image I_i sees element E_j well enough, or conversely element E_j is seen in image I_i well enough. This relation is built from the image point of view as for each image we define which elements are seen well enough. However, we usually need the inverse information: for the scene element on which we want to focus our method, which image should we use? This requires to build a visibility graph containing two types of nodes (image and scene elements). Each visibility relation will be an edge in this graph between an image and an element node, that will be registered from both image and edge point of view. Constructing this graph is required to inverse the visibility information, but it is also useful for optimization and optionally for further simplification. A visualization of this visibility graph is proposed in Fig. 3.

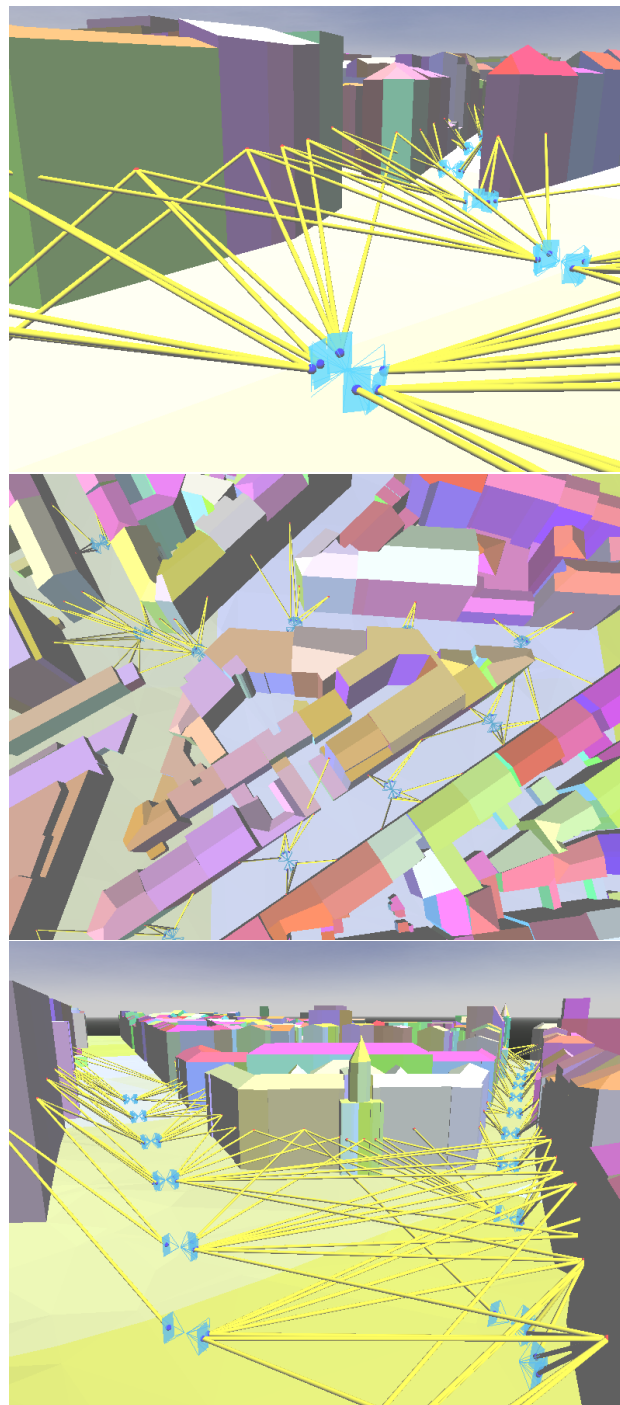


Figure 3: Various views of the visibility graph computed on our test scene (for clarity, only 10% of the images were used). Image (resp. scene) nodes are displayed in blue (resp. red).

3.3 Optimizing memory handling

The visibility graph allows to cut a reconstruction/texture mapping problem into sub-problems by inputting only the images seeing a scene element well enough. A trivial approach to process an entire scene sequentially is to load all these images when processing each scene element, then free the memory before processing the next element. This trivial approach is optimal in terms of memory footprint, but an image seeing N scene elements will be loaded N times, which increases the overall computing time, especially if the images are stored on a Network Attached Storage (NAS). Using a NAS is common practice in mobile mapping as

Dataset	#walls	#images	path length
Ours	4982	5344 (334x16)	1km
Bénitez	11408	1980 (990x2)	4.9km

Table 1: Comparison between our dataset and the dataset of Bénitez.

an acquisition produces around one TeraByte of (uncompressed) image data per hour. The optimization we propose is useful if the loading time is not negligible compared to the processing time, and if the network is a critical resource (in case images are on a NAS). It consists in finding the appropriate order in which to process the scene elements in order to load each image only once. The algorithm is based on the visibility graph, where additional information will be stored in each node (loaded or not for images, processed or not for scene elements):

1. Select any scene element E_j in the scene as starting point of the algorithm and add it to a set S_a of "active elements".
2. For each image I_i^j viewing E_j , load it and add the unprocessed elements seen by I_i^j to S_a .
3. Process E_j , mark E_j as processed and remove it from S_a .
4. If an I_i^j has all its viewed elements processed, close it.
5. Select the element E_j with fewest unopened seeing images in S_a .
6. While S_a is not empty, go back to 2.
7. If no unprocessed element remain, terminate.
8. Select an unprocessed element E_j and go back to 2,

This algorithm is quite simple to implement once the visibility graph has been created, and will be evaluated in Section 4.

3.4 Sequence selection

Another useful utilization of the visibility graph is *sequence selection*. In practice, we found out that images acquired by a mobile acquisition device are often redundant, as the coverage of an entire city require to traverse some streets more than once. Most georeferencing devices use an inertial central allowing for very precise relative localization but can derive due to GPS masks. Hence redundant image sequences viewing the same scene element usually have a poor relative localization. Moreover, the scene may have changed between two traversals: parked cars gone, windows closed, shadows moved... In consequence, we propose to cluster the set of images seeing a given scene element according to their time of acquisition, then select the cluster (sequence) with the best quality (using the criteria of Section 3.1).

4 RESULTS AND DISCUSSION

We have developed the tools described in this paper in order to perform large scale reconstruction and texture mapping of various urban objects such as facades, trees,... However, this paper only focuses on the optimized visibility computation, that is a mandatory prerequisite for such applications. Consequently, the results presented in this section consist mainly in statistics and timings demonstrating the quality efficiency of our approach.

The method presented in this paper (rasterization) was evaluated on a set of images acquired in a dense urban area with the mobile mapping system of (Bentrah et al., 2004). The set consists



Figure 4: Visualization of the 5344 images used in our experiments.

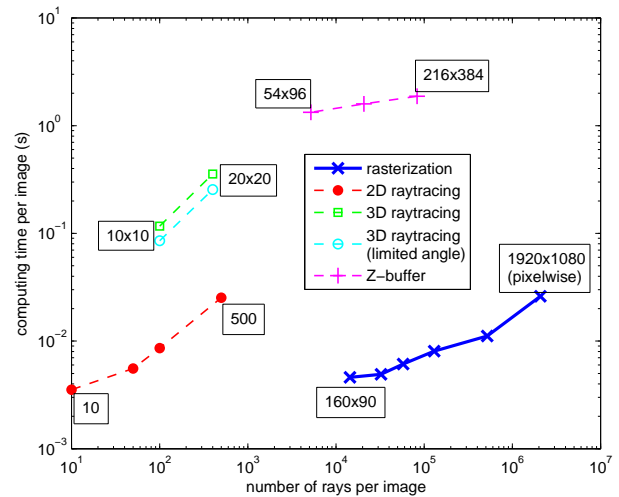


Figure 5: Timings for visibility computation. Results are compared between our rasterization approach (thick blue line) with subsampling factors ranging from 1 to 24, and the three approaches of Bénitez (dotted lines).

of 334 vehicle positions, every 3 meters along a 1km path. For each position, 16 images were acquired (12 images forming a panoramic + 2 stereo pairs). We also disposed of a 3D city model of the acquired area built from aerial imagery. Comparison with the dataset of (Bénitez and Baillard, 2009) is displayed in Table 1. The main difference is that our path is shorter, but our image density is much higher. The images acquired are represented inserted in the 3D model on Fig. 4.

The timings for the computation of the visibility graph running on an NVidia GeForce GTX 480 are presented on Fig. 5, along with equivalent timings taken from (Bénitez and Baillard, 2009). They are given with respect to the number of visibility queries computed per image (number of rays traced or of buffer pixels). A high number of rays ensures that most visibility relationships will be found (good angular precision).

As expected, the use of the GPU allows for a huge performance increase for 3D visibility computation, even though our results are much more accurate: for an equivalent number of rays, our rasterization approach is around 400 times faster than Z-buffering. This huge performance increase is however limited to high ray numbers, as decreasing the resolution of our rasterization does

min area	max pix size	image/wall	mode	max footprint	#image loads
0	∞	39.2	trv. opt.	414 1854	52085 5058
1%	$(10cm)^2$	28.7	trv. opt.	191 521	9644 3811
2%	$(4cm)^2$	20.1	trv. opt.	120 242	5337 2886
5%	$(2cm)^2$	13.9	trv. opt.	44 51	2665 1793

Table 2: Influence of geometric criteria on visibility graph density, and comparison of memory footprint and loading times between trivial (trv.) and optimized (opt.) processing.

not improve the computing time below 10^4 rays. Some steps of the rendering pipeline have a computation time depending on the number of primitives of the scene and not on the size of rendering, which explains the limit we reach (around 4.6ms per image) for low resolutions. Even though our computing time does not improve below 10^4 rays, it is still 20 times faster (for 160×90 rays) than 10×10 3D ray tracing.

The only method of (Bénitez and Baillard, 2009) with performance comparable to ours is 2D ray tracing. In our sense, this method is not suitable in urban areas in which configurations requiring the third dimension are often encountered (such as a taller building behind a smaller one). This is confirmed by (Bénitez and Baillard, 2009) who found that 2D ray tracing misses one third of the walls (compared to Z-buffering). Moreover, they state that 100 rays per image is a good compromise. For this number of rays, 2D ray tracing is already slower than our rasterization.

Finally, our approach is clearly the only one allowing for pixelwise visibility computation in reasonable time (26ms per image, rightmost point of Fig. 5). It can even be brought down to 20ms per image with the color counting acceleration described in Section 3.1. This high performance makes pixelwise visibility image computation time of the same order of magnitude than image loading time (15ms in our experiments), so the visibility images can be computed on the fly when required instead of being precomputed and saved, which is another nice performance improving feature of our approach.

Finally, we evaluated the optimized memory handling by creating four visibility graphs of different densities by imposing increasingly harsh geometric constraints (see Table 2). As expected, optimized processing greatly reduces the number of loads (each image is loaded exactly once) at the cost of memory footprint (maximum number of images loaded simultaneously), and this effect is more important on denser graphs. If memory size is a limit and/or processing time is large compared to data loading time, then the trivial approach should be used. In other cases, and especially if data transfers are the bottleneck, then the optimized method will be preferable. Table 2 also shows that harsher constraints reduces the number of selected images, such that only the most pertinent ones are preserved.

5 CONCLUSIONS AND FUTURE WORK

We have presented a methodology allowing easy scaling of reconstruction and texture mapping methods on large areas. Computing the visibility graph of large scenes becomes tractable based on our approach, even at the pixel level. Enriching 3D models based on large amounts of data acquired at the ground level is becoming a major application of mobile mapping, and we believe that this methodology will prove useful to make the algorithms developed

in this context scalable. Our evaluation shows that our approach outperforms previous works both in quality and computing time.

The method described in this paper is mostly useful for texture mapping purposes where the per pixel visibility information is required in order to predict occlusion of the model by itself. However, it can also be used for unpredictable occlusions by inserting a point cloud corresponding to detected occluders in the 3D scene before rendering. But this method can also be used for any reconstruction method where a rough estimate of the geometry is known (bounding box, point cloud, 2D detection in aerial images,...)

In the future, we will look into optimizing our approach for larger 3D models based on spatial data structures such as octrees in order to load only the parts of the model that are likely to be seen. We will also investigate doing the color counting directly on the GPU to avoid transferring the buffer from graphics memory to RAM.

REFERENCES

- Bénitez, S. and Baillard, C., 2009. Automated selection of terrestrial images from sequences for the texture mapping of 3d city models. In: CMRT09. IAPRS, Vol. XXXVIII, Part 3/W4, pp. 97–102.
- Bénitez, S., Denis, E. and Baillard, C., 2010. Automatic production of occlusion-free rectified faade textures using vehicle-based imagery. In: IAPRS, Vol. XXXVIII, Part 3A (PCV'10).
- Bentrah, O., Paparoditis, N. and Pierrot-Deseilligny, M., 2004. Stereopolis : An image based urban environments modelling system. In: International Symposium on Mobile Mapping Technology (MMT), Kunming, China, March 2004.
- Frueh, C. and Zakhor, A., 2003. Constructing 3d city models by merging ground-based and airborne views. In: Proceedings of the 2003 IEEE Computer Society Conference on Computer Vision and Pattern Recognition (CVPR03).
- Frueh, C. and Zakhor, A., 2004. An automated method for large-scale, ground-based city model acquisition. In: International Journal of Computer Vision, Vol. 60(1), pp. 5–24.
- Haala, N., 2004. On the refinement of urban models by terrestrial data collection. Arch. of Photogrammetry and Remote Sensing, Commission III WG 7 35, pp. 564–569.
- Huang, H., 2008. Terrestrial image based 3d extraction of urban unfoliated trees of different branching types. In: The International Archives of the Photogrammetry, Remote Sensing and Spatial Information Sciences, Vol. XXXVII, Beijing, China.
- Korah, T. and Rasmussen, C., 2008. Analysis of building textures for reconstructing partially occluded facades. In: European Conference on Computer Vision.
- Lothe, P., Bourgeois, S., Dekeyser, F., Royer, E. and Dhome, M., 2009. Towards geographical referencing of monocular slam reconstruction using 3d city models: Application to real-time accurate vision-based localization. In: IEEE Conference on Computer Vision and Pattern Recognition (CVPR'09), Miami, Florida.
- Pénard, L., Paparoditis, N. and Pierrot-Deseilligny, M., 2004. 3d building facade reconstruction under mesh form from multiple wide angle views. In: IAPRS vol. 36 (Part 5/W17), 2005.
- Wang, X., Totaro, S., Taillandier, F., Hanson, A. R. and Teller, S., 2002. Recovering facade texture and microstructure from real-world images. In: Proc. of the 2nd International Workshop on Texture Analysis and Synthesis in conjunction with ECCV'02, pp. 145–149.
- Xiao, J., Fang, T., Zhao, P., Lhuillier, M. and Quan, L., 2009. Image-based street-side city modeling. In: ACM Transaction on Graphics, 28(5), 2009 (also in proceedings of SIGGRAPH ASIA'09).